⌘ *Author's Choice*

THE JOURNAL OF BIOLOGICAL CHEMISTRY VOL. 286, NO. 20, pp. 18056–18065, May 20, 2011

Superoxide Is Produced by the Reduced Flavin in Mitochondrial Complex I

*A SINGLE, UNIFIED MECHANISM THAT APPLIES DURING BOTH FORWARD AND REVERSE ELECTRON TRANSFER**

Received for publication, September 20, 2010, and in revised form, February 23, 2011 Published, JBC Papers in Press, March 10, 2011, DOI 10.1074/jbc.M110.186841

Kenneth R. Pryde and Judy Hirst[1]

From the Medical Research Council Mitochondrial Biology Unit, Wellcome Trust/MRC Building, Hills Road, Cambridge, CB2 0XY, United Kingdom

NADH:ubiquinone oxidoreductase (complex I) is a major source of reactive oxygen species in mitochondria and a contributor to cellular oxidative stress. In isolated complex I the reduced flavin is known to react with molecular oxygen to form predominantly superoxide, but studies using intact mitochondria contend that superoxide may result from a semiquinone species that responds to the proton-motive force (Δp) also. Here, we use bovine heart submitochondrial particles to show that a single mechanism describes superoxide production by complex I under all conditions (during both NADH oxidation and reverse electron transfer). NADH-induced superoxide production is inhibited by complex I flavin-site inhibitors but not by inhibitors of ubiquinone reduction, and it is independent of Δp. Reverse electron transfer (RET) through complex I in submitochondrial particles, driven by succinate oxidation and the Δp created by ATP hydrolysis, reduces the flavin, leading to NAD^+ and O_2 reduction. RET-induced superoxide production is inhibited by both flavin-site and ubiquinone-reduction inhibitors. The potential dependence of NADH-induced superoxide production (set by the NAD^+ potential) matches that of RET-induced superoxide production (set by the succinate potential and Δp), and they both match the potential dependence of the flavin. Therefore, both NADH- and RET-induced superoxide are produced by the flavin, according to the same molecular mechanism. The unified mechanism describes how reactive oxygen species production by complex I responds to changes in cellular conditions. It establishes a route to understanding causative connections between the enzyme and its pathological effects and to developing rational strategies for addressing them.

Complex I (NADH:ubiquinone oxidoreductase) is a major entry point for electrons to the respiratory chain in mammalian mitochondria (1). It oxidizes NADH to NAD^+, reduces ubiquinone to ubiquinol, and uses the redox potential difference to translocate protons across the mitochondrial inner membrane. The translocated protons contribute to the proton motive force (Δp) that supports ATP synthesis and many transport processes. Complex I is a significant source of cellular reactive oxygen species (ROS)[2] also (2). Thus, complex I is associated with many mitochondrial pathologies and neurodegenerative diseases as a result of both decreases in its catalytic capability and increases in its ROS production (3, 4). Defining and characterizing the sites and mechanisms of ROS production by complex I provide a route to understanding causative connections between the enzyme and its pathological effects and to developing rational strategies for addressing them.

In isolated complex I there is substantial evidence that ROS are produced only by the reduced flavin mononucleotide, the cofactor that oxidizes NADH (5). In the presence of NADH only, isolated complex I from *Bos taurus* heart mitochondria reduces O_2 to predominantly superoxide; less than 10% of the O_2 is reduced directly to H_2O_2. The superoxide that is produced dismutates rapidly to produce H_2O_2 (the dismutation step is not rate-limiting) so that the rate of superoxide (and H_2O_2) production by complex I can be quantified accurately by measuring the rate of H_2O_2 production (5). The rate of superoxide production by the flavin in complex I is set by a pre-equilibrium with NADH and NAD^+. The NAD^+/NADH ratio determines the population of complex I molecules that have a fully reduced flavin; the nucleotide concentrations determine the binding site occupancy. Only those molecules that have a reduced flavin in a nucleotide-free binding site react with O_2 in a slow, rate-determining step to form superoxide (and H_2O_2); the reaction is unaffected by ubiquinone oxidation or the binding of Q-site inhibitors (5, 6). Thus, the flavin-site mechanism explains how the composition of the mitochondrial NAD^+ pool may affect ROS production, and clear links between NAD(P)H oxidation state and ROS production have been identified in mitochondria (7, 8). Furthermore, expression of the yeast alternative NADH dehydrogenase in *Drosophila* confers increased lifespan; the NAD^+/NADH ratio is raised, and ROS production and the aging-associated decline in respiratory capacity are mitigated (9).

In contrast, many studies on intact mitochondria have suggested that complex I produces ROS (usually considered as superoxide but detected as H_2O_2 diffusing out of the mitochondria) by a mechanism involving an iron-sulfur cluster that is

* This work was supported by the Medical Research Council.

⌘ *Author's Choice*—Final version full access.

[1] To whom correspondence should be addressed. Tel.: 44-1223-252810; E-mail: jh@mrc-mbu.cam.ac.uk.

[2] The abbreviations used are: ROS, reactive oxygen species; ACMA, amino-6-chloro-2-methoxyacridine; DPI, diphenyleneiodonium; RCR, respiratory control ratio; RET, reverse electron transfer; SMP, submitochondrial particle; SOD, superoxide dismutase; cyt *c*, cytochrome *c*; $APAD^+$, 3-acetylpyridine adenine dinucleotide.

adjacent to the ubiquinone binding site (Q-site) and/or ubisemiquinone intermediates (for review, see Refs. 2 and 10). Originally, the observation that complex I Q-site inhibitors such as rotenone increase H_2O_2 production from mitochondria respiring on NADH-linked substrates was used to propose the involvement of the Q-site (11). However, this observation is readily explained by the flavin-site mechanism, as inhibiting NADH oxidation causes NADH to accumulate and lowers the NAD^+/NADH ratio (lowers the NAD^+ potential). Two further observations have been proposed to be inconsistent with the flavin-site mechanism and to support a semiquinone-based (or related) mechanism (11–13). First, higher rates of H_2O_2 production are observed during reverse electron transport (RET) by mitochondria than during NADH oxidation. RET refers to the reduction of NAD^+ by complex I, driven by succinate oxidation to produce ubiquinol (to supply the electrons), and by a substantial Δp (to overcome the unfavorable redox potential difference) between ubiquinol and NAD^+. The idea is that the flavin can be fully reduced during NADH oxidation; this sets a maximum rate of H_2O_2 production from the flavin that should not be exceeded during RET (13). Second, Δp has two components that represent the difference in charge ($\Delta\psi$) and pH (ΔpH) on each side of the membrane. In mitochondria, their relative contributions can be manipulated, and during both NADH oxidation and RET, H_2O_2 production appears to accelerate as ΔpH increases. The idea is that the flavin is less intimately linked to proton translocation than the Q-site, so it should not be significantly affected by ΔpH (12).

Here, we use submitochondrial particles (SMPs, inverted membrane vesicles) from *B. taurus* heart mitochondria to bridge the gap between studies of superoxide and H_2O_2 production on the isolated enzyme and on intact mitochondria. Like intact mitochondria, our SMPs sustain a substantial Δp during energy-linked forward (NADH or succinate:O_2 oxidoreduction) electron transport, and they catalyze Δp-driven reverse electron transport. Like the isolated enzyme, our SMPs allow precise control over the availability of substrates and the conditions for the active site chemistry, and superoxide and H_2O_2 detection are unaffected by the mitochondrial antioxidant defenses. Our results define an integrated and unified mechanism for superoxide and H_2O_2 production by the reduced flavin in complex I that applies under all conditions and that is relevant to understanding how rates of ROS production by complex I in intact mitochondria are determined.

EXPERIMENTAL PROCEDURES

All chemicals were supplied by Sigma unless otherwise stated.

The Preparation of SMPs from B. taurus Heart Mitochondria—Mitochondria were prepared from *B. taurus* heart tissue as described previously (14) and stored as ~5 g pellets at −20 °C. A single pellet was thawed overnight at 4 °C, resuspended in 10 mM Tris-SO_4, 250 mM sucrose at pH 7.0 (final volume 120 ml, pH corrected at 20 °C, buffer A), and refrozen. 40 ml of suspension (thawed at 4 °C) were centrifuged (11,300 × *g*, 12 min, 4 °C), the dark red supernatant was discarded, and the pellet was resuspended in buffer A to 40 ml; this step helps remove saturated fats as well as soluble proteins. The pH was adjusted to 9 on ice by the dropwise addition of 2.5 M Tris (15), and the sample was incubated on ice for 15 min then recentrifuged (37,900 × *g*, 12 min, 4 °C); this step aims to dissociate the inhibitor protein, IF_1, from ATP synthase (16). The supernatant was discarded, and the pellet was twice resuspended in buffer A to 40 ml and recentrifuged (11,300 × *g*, 12 min, 4 °C). Then 10 mM $MgSO_4$ was added because it improves the respiratory control ratio (RCR) values of the preparation (17, 18), and the sample was sonicated on ice (Sonicator 3000, Misonix, 19 mm probe, ten 15 s bursts with 1 min intervals, 150 Watts). The sonicated material was centrifuged (27,100 × g, 20 min, 4 °C), and the pellet was discarded. Then, 1 mM NADH was added, and the sample was incubated for 1 h on ice; this step aims to activate any complex I that has undergone the "deactive" transition (15). The SMPs were collected by centrifugation (82,000 × *g*, 30 min, 4 °C) then twice resuspended to 4 ml in buffer A and recentrifuged to remove the nucleotides. Finally, the SMPs were resuspended to ~7 mg of protein ml^{-1} (determined using the Pierce bicinchoninic acid (BCA) assay) and stored as aliquots at −20 °C. The yield was typically ~30 mg of protein of SMPs.

Catalytic Activity Measurements—All kinetic measurements were performed in 10 mM Tris-SO_4, 250 mM sucrose at pH 7.5, 32 °C, in an Ocean Optics DH-2000-BAL diode array spectrometer, a Molecular Devices spectramax plus 384 plate reader, or a Shimadzu RF-5301 PC spectrofluorometer.

NADH:O_2 oxidoreduction (100 μM NADH) and NADH:fumarate oxidoreduction (100 μM NADH, 40 mM fumarate, 400 μM KCN) were followed at 340–380 nm (ϵ_{NADH} = 4.81 mM^{-1} cm^{-1}). Succinate:O_2 oxidoreduction (20 mM succinate) was followed using a Clark electrode. ATP hydrolysis was followed using a coupled assay to detect ADP (19); ADP drives the conversion of phosphoenolpyruvate (200 μM) to pyruvate by pyruvate kinase (40 μg ml^{-1}), then pyruvate reduction was coupled to NADH oxidation (200 μM) by lactate dehydrogenase (50 μg ml^{-1}). Rotenone was used to prevent NADH oxidation, and the reaction was initiated with 200 μM ATP+$MgSO_4$ and followed at 340–380 nm. ATP hydrolysis traces were biphasic due to a known lag phase from the expulsion of bound ADP (20); reported rates are for the second, linear phase. Succinate:NAD^+ oxidoreduction (RET, in 10 mM succinate, 1 mM NAD^+, 1 mM ATP+$MgSO_4$, 400 μM KCN) was followed at 340–380 nm; assay traces exhibited a short lag phase before becoming linear due either to ATP hydrolysis (see above) or to the reactivation of small quantities of deactive enzyme (15). NADH:ferricyanide, hexaammineruthenium (HAR), and 3-acetylpyridine adenine dinucleotide ($APAD^+$) oxidoreduction (100 μM NADH, 1 mM ferricyanide, 3.5 mM HAR, 1 mM $APAD^+$, rotenone) were followed as described previously (6). Cytochrome *c*:O_2 oxidoreduction (100 μM bovine heart cytochrome *c*, reduced using excess sodium dithionite and purified using a PD10 Sephadex G-25 column) was monitored via the oxidation of the reduced cytochrome *c* (cyt *c*) (see below). The fluorescence of 500 nM amino-6-chloro-2-methoxyacridine (ACMA) was measured using excitation and emission wavelengths of 435 and 477 nm, respectively, typically in the presence of ~100 μg of protein ml^{-1} SMPs.

H_2O_2 and Superoxide Production Measurements—H_2O_2 production was quantified using the horseradish peroxidase

TABLE 1

Catalytic properties of a typical SMP preparation

Reaction 1, 100 μM NADH; reaction 2, 20 mM succinate; reaction 3, 100 μM NADH, 40 mM fumarate, 400 μM KCN; reaction 4, 1 mM NAD^+, 10 mM succinate, 2 mM ATP+$MgSO_4$, 400 μM KCN; reaction 5, 0.2 mM ATP+$MgSO_4$, 23 μM rotenone.

Catalytic reaction	Rate of reaction (μmol min^{-1} mg $protein^{-1}$)		RCR
	Coupled (+Δp)	Uncoupled (Δp = 0)[a]	
1. NADH:O_2 oxidoreduction[b]	0.246 ± 0.011	0.743 ± 0.018	3.02 ± 0.15[c]
2. Succinate:O_2 oxidoreduction	0.148 ± 0.015	0.264 ± 0.024	1.78 ± 0.24
3. NADH:fumarate oxidoreduction	0.052 ± 0.001	0.053 ± 0.001	1.02 ± 0.03
4. Succinate:NAD^+ oxidoreduction (RET)[b,d]	0.133 ± 0.002	0.002 ± 0.002	
5. ATP hydrolysis	0.893 ± 0.109	1.353 ± 0.043	1.52 ± 0.19

[a] Δp was collapsed using 10 μg ml^{-1} gramicidin.

[b] Observed rates of NADH:O_2 and succinate:NAD^+ oxidoreduction varied by up to 2-fold between preparations and were comparable to a range of published values recorded in varying conditions (see for example Refs. 15 and 30). Conversely, the rates of reactions that are catalyzed only by the flavin site in complex I did not vary significantly.

[c] When SMPs were prepared without the NADH incubation to activate them during the preparation (15) several wash steps could be omitted, and the RCR values were significantly higher (5–6 for NADH:O_2 oxidoreduction). These SMPs were not used extensively here because their rates of RET are significantly diminished unless they are pre-activated with NADH, a procedure that results in nucleotides being present in the assay; they were used only for comparison with our standard preparation, in experiments to quantify NADH-induced H_2O_2 production (see "Results").

[d] Activating the complex I with NADH (15) immediately before the RET assay typically increased the rate by 20%, suggesting that ~80% of the complex I is already in the active form.

(HRP)-dependent oxidation of Amplex Red (10 μM, Invitrogen) to resorufin, monitored at 557–620 nm (ϵ = 51.6 ± 2.5 mM^{-1} cm^{-1} at pH 7.5) (5, 7). The HRP concentration was 2 units ml^{-1}, and increased to 8 units ml^{-1} when 400 μM KCN was present; further increasing the concentration did not affect the observed rate. NADH-induced H_2O_2 production was determined in 30 μM NADH (5, 21); E_{Set} was set by varying the NAD^+ concentration. When necessary, the NADH was re-purified by ion exchange chromatography under anaerobic conditions (22). Re-purification was crucial for redox potential titrations and absolute rate measurements (for example, detection of NADH-induced H_2O_2 production by rotenone-inhibited complex I increased from 4.83 ± 0.04 to 5.20 ± 0.09 nmol min^{-1} mg of $protein^{-1}$), but it did not affect comparative measurements or catalytic rate measurements. Unless stated otherwise, rates of NADH-induced H_2O_2 production reported here were determined using re-purified NADH. RET-induced H_2O_2 production was measured in 10 mM succinate, 1 mM ATP+$MgSO_4$, and 400 μM KCN; E_{Set} was set by varying the fumarate concentration. 50 μM acetylated cyt *c* was used for the direct detection of superoxide production by complex I (ϵ = 18.0 mM^{-1} cm^{-1}, 550–541 nm) (5, 23) in 30 μM NADH (NADH-induced) or in 10 mM succinate, 1 mM ATP+$MgSO_4$, and 400 μM KCN (RET-induced).

Catalase was from bovine liver (2–8 units ml^{-1}), and superoxide dismutase (SOD) was the CuZn enzyme from bovine erythrocytes (2 units ml^{-1}). SMP preparations were checked to make sure they did not have the ability to remove H_2O_2 and superoxide from solution and, thus, affect their detection; the rates of H_2O_2 and superoxide production by xanthine oxidase (Fluka, 0.94 milliunits ml^{-1} + 10 μM xanthine) (24) were measured in the presence and absence of SMPs (140 μg ml^{-1}). The SMPs made no significant difference to the detection (by the Amplex Red system) of the H_2O_2 produced (in the presence or absence of SOD), so they do not have any significant ability to remove H_2O_2. SMPs also did not affect the detection of standard concentrations of H_2O_2 added directly to assay solutions. In the presence of KCN, SMPs made no significant difference to the detection (by acetylated cyt *c*) of the superoxide produced, so they did not have any significant ability to remove superoxide from the solution either; they do not contain detectable SOD activity. The KCN was added to prevent the reoxidation of reduced cyt *c* by cytochrome *c* oxidase, a reaction that decreases detection of the superoxide.

Inhibition of the Respiratory Chain Enzymes and Dissipation of Δp—Rotenone (23 μM) and piericidin A (10 μM) were used to inhibit complex I (>99% inhibition of NADH:O_2 oxidoreduction) and NADH-OH (2.5 μM, >99%) (25) and ADP-ribose (5 mM, >80%) (26) to competitively inhibit the complex I flavin site. Diphenyleneiodonium chloride (DPI) is a noncompetitive inhibitor that reacts irreversibly with the reduced flavin (27); the DPI concentration and incubation time were adjusted for the experimental conditions (high NADH concentrations prevent DPI from accessing the reduced flavin). Malonate (a competitive inhibitor of succinate oxidation, 20 mM, >99% inhibition of succinate:O_2 oxidoreduction) (28) and carboxin (20 μM) were used to inhibit complex II. Carboxin binds to the quinone site in complex II (29); its solubility in ethanolic stock solutions limits its concentration in the assay to 20 μM (~60% inhibition). All inhibitors were checked for artifacts in the Amplex Red assay; antimycin A, a Q_i site inhibitor of complex III, was used at 500 nM (~94% inhibition of NADH:O_2 oxidoreduction) because higher concentrations interfere with the Amplex Red assay; myxothiazol was not used because it also inhibits complex I (11) and because it leads to artifactual H_2O_2 detection. 400 μM KCN was used to inhibit cytochrome *c* oxidase (~98% inhibition of NADH:O_2 oxidoreduction); the KCN concentration was minimized to minimize HRP inhibition. Gramicidin (mixture of forms A, B, C, and D, 10–40 μg ml^{-1} depending on the SMP concentration) was used to dissipate Δp. FCCP (carbonyl cyanide 4-(trifluoromethoxy)phenylhydrazone) was not used because its effect is concentration dependent; as the concentration increases, the rate of NADH:O_2 oxidoreduction first increases, but before a maximum rate is attained it decreases again.

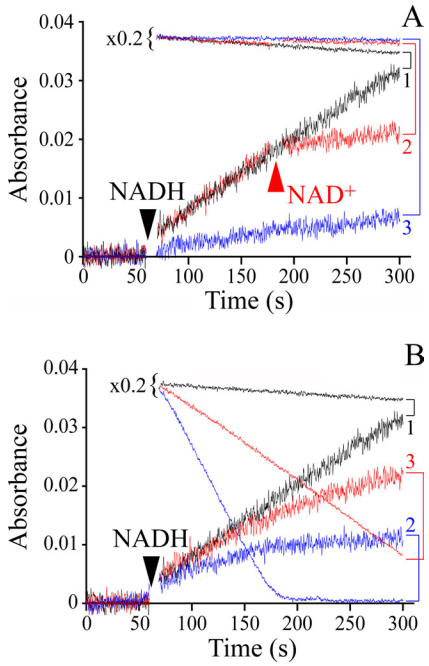

FIGURE 1. **Measurements of H_2O_2 production and NADH oxidation by complex I in SMPs.** H_2O_2 production (measured by the accumulation of resorufin, *y* axis scale) by SMPs (35 μg of protein ml^{-1}) was initiated by 30 μM NADH, and NADH oxidation was measured alongside (the intensity of the NADH traces has been multiplied by 0.2). *A*, in the presence of rotenone, H_2O_2 production and NADH oxidation were linear (*black traces*, *1*). 1 mM NAD^+ (*red traces*, *2*) decreased both rates to the background level recorded in the presence of DPI (*blue traces*, *3*). *B*, the *black trace* (*1*) is reproduced from *panel A*. The *blue trace* (*2*) was recorded during catalytic NADH oxidation (no inhibitor) with $\Delta p = 0$ (in the presence of gramicidin). The *red trace* (*3*) was recorded during NADH oxidation in the presence of Δp. The H_2O_2 production traces (*2B* and *3B*) curve in response to NADH oxidation. See "Experimental Procedures" for conditions.

RESULTS

SMPs as a Model System for Studying Energy Transduction in the Inner Mitochondrial Membrane—Table 1 summarizes the kinetic properties of a typical SMP preparation. NADH:O_2 and succinate:O_2 oxidoreduction and ATP hydrolysis are all energy-conserving reactions (coupled to proton translocation), so their rates increase significantly when Δp is dissipated. NADH:fumarate oxidoreduction is also energy conserving, but it is probably limited kinetically by quinol:fumarate oxidoreduction. Both the reaction rates and their RCRs (the ratio of the rates in the presence and absence of Δp, which reflect the ability of the system to work against Δp as well as how well the vesicles are sealed) are comparable with values described previously (see for example Refs. 15 and 30) and consistent with a population of catalytically active, well coupled particles.

Importantly, both ATP hydrolysis and NADH:fumarate oxidoreduction can be "reversed" by using Δp to drive them away from equilibrium. Initial experiments showed that NADH oxidation can drive ATP synthesis to more than 90% completion (quantified by the luciferase assay, 200 μM ADP, 10 mM potassium phosphate, 10 mM $MgSO_4$, 70 μg ml^{-1} IF_1 (31)), showing that NADH oxidation supports a substantial Δp. NAD^+ reduction driven by succinate oxidation (to reduce the ubiquinone pool) and ATP hydrolysis (to create Δp) proceeds by RET through complex I, and the fact that it achieves a significant rate (see Table 1) demonstrates that a substantial Δp is sustained (32). By including an NADH activation step in our preparation (see "Experimental Procedures"), our SMPs were optimized for a maximum rate of RET without requiring nucleotides to be added to the assay buffer to activate the deactive form of complex I *in situ* (15). In addition, we avoided stimulating RET by adding poorly defined and complicating couplers or activators, such as oligomycin (15) or fatty-acid-free bovine serum albumin (which interferes with both the ACMA and Amplex Red detection systems also) (15). Finally, all the catalytic activities in Table 1 are sensitive to the canonical respiratory chain inhibitors rotenone and piericidin A (complex I), malonate and carboxin (complex II), antimycin A (complex III), and cyanide (complex IV), and RET is abolished by uncoupling agents also.

NADH-induced Superoxide and H_2O_2 Production by Complex I in SMPs—Fig. 1 shows a set of experiments that monitored both NADH-induced H_2O_2 production and NADH oxidation by complex I in SMPs. The addition of NADH initiates H_2O_2 production. If catalysis (energy-transducing NADH:O_2 oxidoreduction) is prevented by rotenone (Fig. 1*A*), then H_2O_2 production is constant, although NAD^+ decreases its rate significantly, to the catalase-insensitive background level observed upon the addition of a complex I flavin-site inhibitor such as DPI (see Table 2). Alternatively, during the catalytic conversion of NADH to NAD^+, H_2O_2 production gradually slows (Fig. 1*B*); the effect was observed in both the presence of Δp and when $\Delta p = 0$. Importantly, the initial rates observed during catalysis match the rate observed when catalysis was inhibited (although the curvature makes them difficult to quantify). Therefore, H_2O_2 production is not stimulated by ubiquinone reduction at the Q-site, for example by the formation of a short-lived semiquinone intermediate (even in the presence of a substantial Δp), or by rotenone binding.

Observed rates of NADH-induced H_2O_2 production were linearly dependent on SMP concentration and were ~80% sensitive to catalase (see Table 2). They were stimulated <10% by SOD (see Table 2) because (as observed previously for purified complex I (5)) even in the absence of SOD the dismutation of superoxide to H_2O_2 is not rate-limiting. The catalase-insensitive rate matches the rates observed in DPI and high concentrations of NAD^+ (see Table 2). It is decreased (but not abolished) in the absence of SMPs and abolished by the absence of HRP or NADH. Thus, it probably represents a direct interaction between NADH and the Amplex Red detection system (21).

Table 2 presents a side-by-side comparison of NADH-induced H_2O_2 and superoxide production by complex I inhibited by rotenone. Superoxide production rates were measured using the reduction of acetylated cyt *c* (5); Table 2 shows that there is a significant DPI-, NAD^+-, and SOD-insensitive component. However, subtraction of the background rates (for both H_2O_2 and superoxide production) led to a ratio of 1.71 ± 0.12 superoxides per H_2O_2. The ratio is lower than 2 (the value expected if complex I only produces superoxide directly) for two reasons. First, the reduced flavin site in purified complex I was shown previously to convert up to 10% of the O_2 consumed directly to H_2O_2 (5). Second, the apparent rate of superoxide production by SMPs is decreased slightly by reoxidation of the reduced cyt

TABLE 2
Side-by-side comparison of measurements of H_2O_2 and superoxide production by a typical SMP preparation

	NADH-induced reactions						
	Obs. value[1]	+ DPI (%)[2]	+ NAD^+ (%)[2]	+ Cat (%)[2]	+ SOD (%)[2]	Corr. value[3]	Complex I[4]
H_2O_2	5.9 ± 0.2	16.5 ± 1.0	11.5 ± 1.2	18.1 ± 1.7	108.7 ± 2.7	4.93 ± 0.2	59.2 ± 2.7
Superoxide	19.1 ± 0.4	55.7 ± 0.1	58.5 ± 0.7		54.2 ± 1.8	8.50 ± 0.2	101.5 ± 2.4[5]
	RET-induced reactions						
	Obs. value[1]	+ DPI (%)[2]	+ Rot (%)[2]	+ Cat (%)[2]	+ SOD (%)[2]	Corr. value[3]	Complex I[4]
H_2O_2	0.39 ± 0.01	49.1 ± 4.7	48.8 ± 2.4	20.0 ± 3.4	102.8 ± 3.5	0.20 ± 0.02	23.8 ± 2.9
Superoxide	2.97 ± 0.02	89.2 ± 1.3	89.5 ± 1.3		88.0 ± 1.6	0.32 ± 0.04	38.5 ± 4.9[5]

[1] The observed (Obs.) values are rates of resorufin formation or rates of acetylated cytochrome *c* reduction and are reported in nmol min^{-1} mg of $protein^{-1}$. The conditions were 30 μM NADH and 23 μM rotenone (NADH-induced) and 10 mM succinate, 2 mM ATP+$MgSO_4$, and 400 μM KCN (RET-induced).
[2] Values are expressed as a percentage of the observed value. NAD^+: 1 mM NAD^+ was added to set the potential to −0.29 V; at this potential superoxide/H_2O_2 formation by the reduced flavin is minimized (5) (see text). Cat, catalase; Rot, rotenone.
[3] The corrected (Corr.) values (nmol min^{-1} mg of $protein^{-1}$) are the observed values adjusted for the background rate (the background rates used here are the DPI insensitive rates). Note that the corrected value reported for NADH-induced H_2O_2 production is slightly lower than the value reported in the text because the NADH used here was not re-purified before use (see "Experimental Procedures").
[4] The complex I rate (min^{-1}) is the rate of superoxide or H_2O_2 production by complex I (the corrected value has been adjusted for the complex I concentration, vesicle orientation, and for RET, for the presence of uncoupled particles, see "Results").
[5] The ratios between the rates of superoxide and H_2O_2 production are 1.71 ± 0.12 (NADH) and 1.62 ± 0.46 (RET). Note that the addition of KCN to the NADH-induced superoxide measurements causes the ratio to increase slightly to ~1.9, because the (slow) reoxidation of reduced cytochrome *c* by cytochrome *c* oxidase is prevented (see "Results").

c by cytochrome *c* oxidase. The addition of KCN prevents the reoxidation reaction, and the measured superoxide:H_2O_2 ratio increases to ~1.9 (note that this value also includes correction for a slow, superoxide-independent change to the cyt *c* spectrum caused by KCN). The data in Table 2 show that measuring H_2O_2 production by complex I is a reliable method of quantitating the total rate of superoxide and H_2O_2 production together and that the H_2O_2 results predominantly from superoxide dismutation. Most of the data presented here are measurements of rates of H_2O_2 production; thus, they are termed "H_2O_2 production" but include both the H_2O_2 produced by superoxide dismutation and the relatively small amount of H_2O_2 produced directly.

Fig. 2 (Δp = 0) shows that complex I produces H_2O_2 at the same rate in the presence of rotenone or piericidin A, inhibitors of ubiquinone reduction by complex I, but in the presence of DPI (27), ADP-ribose (6, 26) and NADH-OH (25), inhibitors of NADH oxidation, the rate is much lower. Antimycin A leads to a higher rate due to a known contribution from complex III (33), as does KCN (the KCN effect was abolished by carboxin so the extra H_2O_2 originates from complex II); both effects were abolished by rotenone.

Fig. 3 compares H_2O_2 production by isolated complex I in the absence of ubiquinone (5) with that by rotenone-inhibited SMPs (the most analogous condition), as a function of the NAD^+ potential. Because the flavin reacts much more rapidly with NADH and NAD^+ than with O_2, the curves in Fig. 3 are essentially redox titrations of the flavin cofactor (5). The data from the two systems match closely, and the values determined for the flavin reduction potential (−0.353 V (isolated complex I) and −0.363 V (SMPs, Δp = 0)) are close to the independent value from EPR (−0.365 V) (34). These data confirm that the flavin-site mechanism described previously for NADH-induced H_2O_2 production by isolated complex I (5, 6) applies equally to complex I in SMPs.

The rate of H_2O_2 production by rotenone-inhibited complex I in SMPs (5.20 ± 0.09 nmol of min^{-1} mg of $protein^{-1}$ after correction for the NADH-OH insensitive rate; see Fig. 2) was

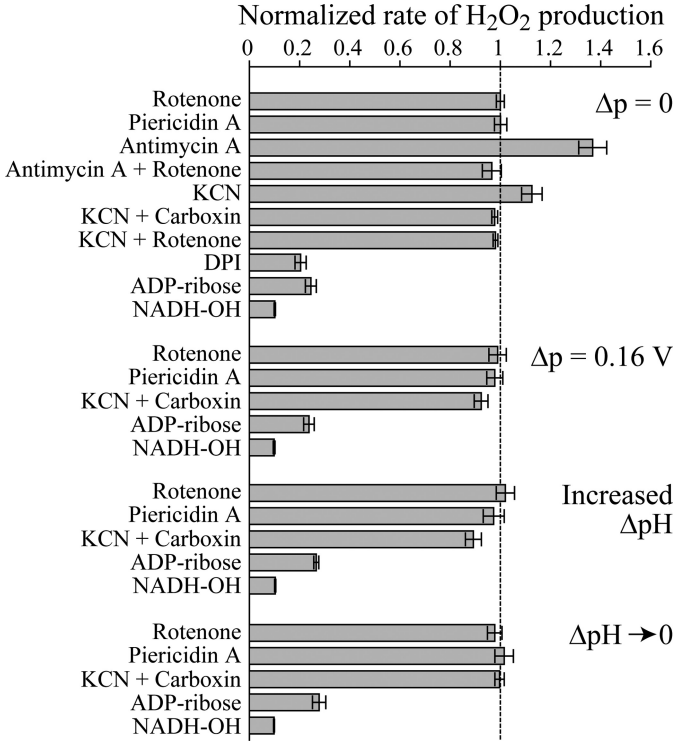

FIGURE 2. **NADH-induced H_2O_2 production in the presence of various respiratory chain inhibitors, in the presence and absence of Δp and ΔpH.** H_2O_2 production was induced by 30 μM NADH and measured using the HRP-Amplex Red system; Δp was imposed by ATP hydrolysis. ΔpH was increased using 20 mM KCl or decreased using 20 mM KCl and 2 nM nigericin (see "Results"). See "Experimental Procedures" for conditions.

adjusted for the orientation of the vesicles and the complex I content. First, the NADH:$APAD^+$ and cytochrome *c*:O_2 oxidoreductase activities were determined before and after solubilization of the SMPs with 0.5% dodecylmaltoside. In a typical experiment the NADH:$APAD^+$ oxidoreductase activity (a reaction catalyzed by the complex I flavin (35)) increased from 1.10 ± 0.01 to 1.30 ± 0.02 μmol of min^{-1} mg of $protein^{-1}$, and the cytochrome *c*:O_2 oxidoreductase activity increased from 1.83 ± 0.01 to 8.37 ± 0.21 μmol min^{-1} mg of $protein^{-1}$. There-

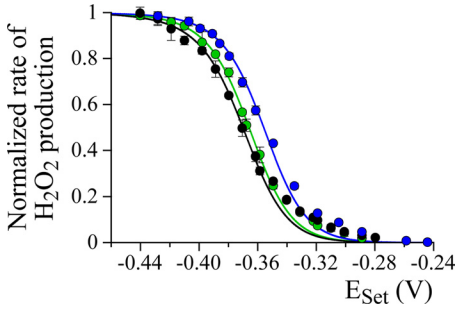

FIGURE 3. **NADH-induced H_2O_2 production by complex I in SMPs with and without Δp compared with that by isolated complex I.** The three curves have been normalized independently. The data are plotted using $E_{Set} = -0.335\ V - RT/2F \cdot \ln\{[NADH]/[NAD^+]\}$ (using 30 μM NADH and variable NAD^+) and fit by the Nernst equation for a 2-electron cofactor with 2 distinct potentials described by their average value, E_{av}, and their separation, Δ*E*. *Blue*, isolated complex I ($E_{av} = -0.353$, ΔE = 0.079 V) (5). *Green*, complex I in SMPs inhibited by rotenone (Δp = 0 V) ($E_{av} = -0.363$, Δ*E* = 0.079 V). *Black*, complex I in SMPs inhibited by rotenone with Δp ~ 0.16 V (generated by ATP hydrolysis) ($E_{av} = -0.366$, Δ*E* = 0.060 V). The NADH-OH independent rates, measured in NADH only (see Fig. 2), have been subtracted from the SMP data sets. See "Experimental Procedures" for conditions.

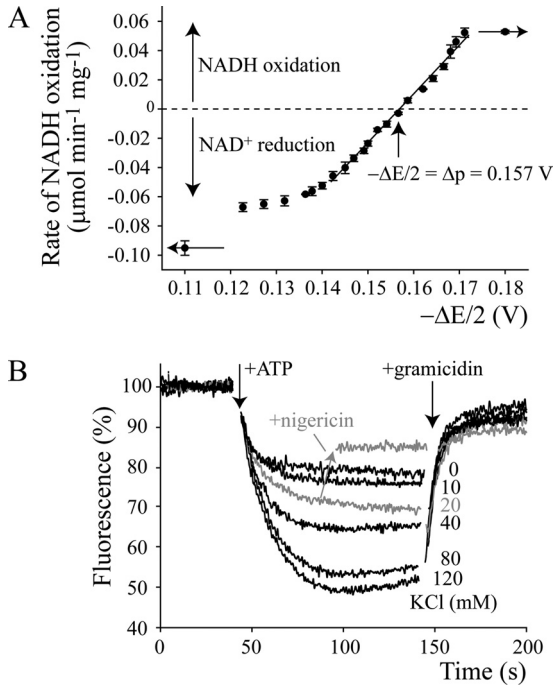

FIGURE 4. **Measurement of Δp in SMPs hydrolyzing ATP and evaluation of ΔpH.** *A*, the rate of NADH:fumarate oxidoreduction, recorded during ATP hydrolysis (1 mM ATP + $MgSO_4$) to generate Δp and with 400 μM KCN to inhibit respiration depends on the difference between the NAD^+ and fumarate potentials, $\Delta E = -0.335\ V + 0.020 - RT/2F \cdot \ln\{([NADH][fumarate])/([NAD^+][succinate])\}$, set using [NADH] = 0.1 mM, [NAD^+] = 1 mM, [succinate] = 0.5 mM, and [fumarate] = 0.025–40 mM. The rate is 0 when $-2\Delta E = 4\Delta p$. When $-2\Delta E$ is close to 4Δp, the data vary linearly with potential, but at high and low potential the rates are determined kinetically; the points with *arrows* are in principal at infinite potential ([NADH] = [fumarate] = 0 shown at 0.11 V, [NAD^+] = [succinate] = 0 shown at 0.18 V). Similar titrations varying the succinate, NAD^+, and NADH concentrations gave, overall, Δp = 0.162 ± 0.005 V. *B*, the fluorescence of ACMA (500 nM) is quenched upon the addition of 100 μM ATP + $MgSO_4$ to SMPs (112 μg ml^{-1}) in varying KCl concentrations. 2 nM nigericin (a K^+/H^+ exchanger) or 20 μg ml^{-1} gramicidin (a cation transporter) abolish the quenching effect. Note that the ACMA fluorescence is affected by ATP (the final value varies). See "Experimental Procedures" for conditions.

fore, the SMP preparations used are 81 ± 5% in the N-side out orientation (reversed with respect to mitochondria). Second, two methods were used to show that complex I comprises ~10% of the total protein in SMPs. First, the intensities of the bands observed in Western blots of the 24- and 51-kDa complex I subunits, from a range of SMP and complex I concentrations, were compared, indicating that complex I comprises 9.1 ± 2.6% of the total protein. The proteins were separated by SDS-PAGE, then transferred to nitrocellulose membranes, labeled with polyclonal antibodies raised against the overexpressed *B. taurus* subunits, and detected by enhanced chemiluminescence. Second, comparison of the intensities of the g_z components of the N2 EPR signal (36) exhibited by samples reduced by 10 mM NADH and inhibited by 10 μM piericidin A from intact complex I and SMPs indicated that 10.1 ± 0.5% of the protein present in SMPs is complex I. Correcting for the orientation and amount of complex I present (~9.6% of the total protein) gave a turnover rate for NADH-induced H_2O_2 production (per complex I) of ~64 min^{-1}. The value (per complex I) is approximately twice as high as the corresponding value from isolated complex I (5, 6), but the rates of three other flavin-catalyzed reactions (6), the NADH:ferricyanide, NADH:$APAD^+$, and NADH:hexaammineruthenium oxidoreductase reactions, are also all approximately twice as high in SMPs compared with isolated complex I. The reason for the difference is not known, but it is likely that SMPs are the most physiologically relevant, because isolating the complex I from SMPs decreased its activity to that of the directly purified enzyme.

The Effects of Δp and ΔpH on NADH-induced H_2O_2 Production—Fig. 1*B* indicated that Δp does not affect the rate of NADH-induced H_2O_2 production when it is generated by catalytic NADH oxidation. Alternatively, the Δp generated by ATP hydrolysis is independent of the respiratory chain. To quantify the Δp from ATP hydrolysis, the potential for NADH:fumarate oxidoreduction (Δ*E*) was varied (by varying the four substrate concentrations according to the Nernst equation), and the potential of zero net rate, at which $-2\Delta E = 4\Delta p$ (each two-electron NADH oxidation translocates four protons) was identified. Fig. 4*A* presents a typical titration that gave Δp = 0.157 V; Δp varied by less than 10 mV between preparations. Our value is similar to the Δp produced by ATP hydrolysis in mitochondria, which was reported to increase NADH-induced H_2O_2 production by rotenone- and piericidin A-inhibited complex I (~0.15 V) (11); clearly, our value is high enough that any Δp-dependent effects on complex I observed in mitochondria should be observed here also. Fig. 2 (Δp = 0.16 V) shows how Δp affects NADH-induced H_2O_2 production by SMPs in the presence of various inhibitors. With rotenone or piericidin A (to prevent quinone reduction by complex I directly) or KCN and carboxin (to prevent complex I turnover indirectly), H_2O_2 production is unaffected by Δp. As expected, ADP-ribose and NADH-OH essentially abolish H_2O_2 production. In addition, NADH-induced H_2O_2 production from SMPs that had higher RCR values because they were not activated by NADH during the preparation (see Table 1) was quantified both in the presence and absence of complex I Q-site inhibitors; the results were fully consistent with the results from our standard preparations. Finally, Fig. 3 shows that the potential dependence of NADH-induced H_2O_2 production from rotenone-inhibited SMPs is independent of Δp. Thus, these results provide no evidence to

support the participation of a second (non-flavin) site of H_2O_2 production.

To investigate the effects on H_2O_2 production of modulating the ΔpH component of Δp, a fluorescent aminoacridine dye (ACMA) was used to evaluate ΔpH. The fluorescence of ACMA is quenched when it partitions into the SMP lumen in response to ΔpH (37, 38). Fig. 4*B* shows how the ACMA fluorescence is quenched by SMPs catalyzing ATP hydrolysis (NADH and succinate oxidation provide similar traces). The ATP concentration was kept to a minimum (100 μM ATP+$MgSO_4$) because ATP itself quenches the fluorescence. Under our standard conditions (0 mM KCl) the fluorescence is quenched by only ~20%, and ΔpH is relatively low. For perfectly sealed particles, transferring just a few protons into the lumen is sufficient to produce a large $\Delta\psi$ without affecting the internal pH, so $\Delta p = \Delta\psi$ and $\Delta pH = 0$. However, when other ions cross the membrane they collapse $\Delta\psi$ (the impediment to proton uptake) so protons accumulate inside; $\Delta\psi$ is converted to ΔpH. Thus, permeant anions were added to the external solution to induce conversion of $\Delta\psi$ to ΔpH. Thiocyanate, an intrinsically membrane permeable anion, could not be used because it dramatically quenches the ACMA fluorescence directly. However, both chloride and nitrate gave similar results (37, 38); it is possible that they are conducted across the membrane by an anion transporter (39). Fig. 4*B* shows that chloride induces the formation of ΔpH with a rate and magnitude dependent on its concentration (37). Conversely, in the presence of K^+, ΔpH can be significantly decreased (perhaps abolished) by nigericin, a K^+/H^+ exchanger. 20 mM KCl ($\Delta\psi$ to ΔpH) and 20 mM KCl + 2 nM nigericin (ΔpH to $\Delta\psi$) were chosen as standard conditions here because they do not affect Δp significantly (determined as in Fig. 4*A*), or decrease the rate of RET by more than 10%.

Importantly, ACMA provides only a qualitative measure of ΔpH; the extent of quenching is strongly dependent on the concentrations of both ACMA and SMPs, and our attempts to calibrate the response by soaking the SMPs in low pH buffers to create an artificial ΔpH were not successful. Furthermore, the simple volume/volume partition equation that has been applied previously (37) leads to a calculated ΔpH of 4.3 pH units in 120 mM KCl, a value that far exceeds Δp. Thus, we adopted a simple and pragmatic approach to estimate ΔpH; we assumed that the maximum quench, in 120 mM KCl, represents the limiting condition $\Delta pH = \Delta p = 0.157$ V (2.6 pH units) and used a linear function (set to ΔpH = 0 in KCl and nigericin) to estimate ΔpH. Our standard conditions are, thus, ΔpH ~ 0.08 V and $\Delta\psi$ ~ 0.08 V (20 mM KCl) and ΔpH ~ 0 V and $\Delta\psi$ ~ 0.16 V (20 mM KCl + 2 nM nigericin). These ΔpH values are maximum estimates because RET cannot be observed in 120 mM KCl, so Δp is probably decreased, and $\Delta\psi$ may not be completely converted to ΔpH (40). Fig. 2 shows that altering the balance between ΔpH and $\Delta\psi$ while keeping Δp and the external pH constant does not affect NADH-induced H_2O_2 production by complex I.

H_2O_2 Production during RET—RET-induced H_2O_2 production was quantified in the absence of NAD^+ using nucleotide-free SMP preparations because bound nucleotides prevent O_2 access, NAD^+ reacts with the reduced flavin, and NADH formation leads to NADH-induced H_2O_2 production by poorly coupled particles. The observed rate of RET-induced H_2O_2 production (with $\Delta p = 0.16$ V, sufficient for substantial NAD^+ reduction; see Table 1) was low in comparison to the NADH-induced rate, only 0.35 ± 0.11 μmol min^{-1} mg of $protein^{-1}$. Table 2 shows that the H_2O_2 detected was not affected significantly by SOD (superoxide dismutation is not rate-limiting) and that it was ~80% sensitive to catalase. However, only around half of the observed rate is DPI- and rotenone-sensitive (see Table 2 and Fig. 5), indicating that the actual rate of RET-induced H_2O_2 production by complex I is only 0.18 ± 0.06 μmol min^{-1} mg of $protein^{-1}$. The rotenone-insensitive contribution does not depend on Δp, but it is sensitive to malonate (therefore, it originates at complex II and/or complex III). Importantly, the rotenone-sensitive contribution is essentially abolished by the flavin site inhibitors NADH-OH, ADP-ribose, and DPI, observations that are consistent only with RET-induced H_2O_2 production being from the flavin site in complex I. Table 2 shows also that RET-induced superoxide production corresponds to H_2O_2 production (within the error of the measurements and taking into account the high background rates of cyt *c* reduction). Therefore, during RET, complex I produces predominantly superoxide, and (as for NADH-induced H_2O_2 production) the rates of H_2O_2 detection described include both the H_2O_2 formed by superoxide dismutation and the H_2O_2 produced directly.

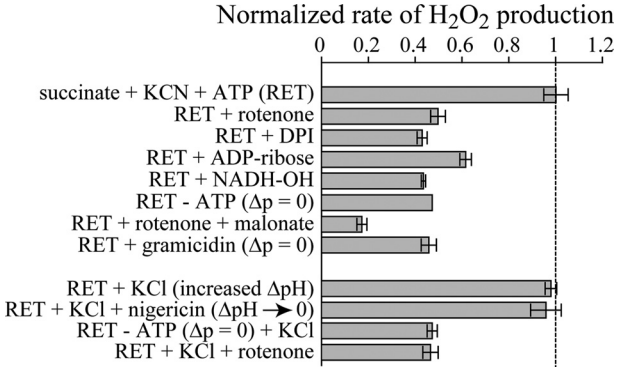

FIGURE 5. **H_2O_2 production during RET in the presence of various respiratory chain inhibitors and in the presence and absence of Δp and ΔpH.** H_2O_2 production rates were measured using the HRP-Amplex Red detection system during the linear phases of the reactions and normalized to the value from the standard RET condition (20 mM succinate, 1 mM ATP+$MgSO_4$, KCN). Δp was collapsed with gramicidin, and ΔpH increased using 20 mM KCl or decreased using 20 mM KCl and 2 nM nigericin (see "Results"). See "Experimental Procedures" for conditions.

Two known effects decrease the rate of RET-induced H_2O_2 production in our experiments. First, because we exclude nucleotides from our experiments, not all of the complex I is in the active form. Second, due to variations in their size, integrity, and enzyme distribution, individual SMPs within a population sustain different Δp values; Δp determined as in Fig. 4*A* is a weighted average. Only some SMPs sustain a high enough Δp to reduce the flavin in complex I, and only those SMPs are able to reduce NAD^+ or O_2. Therefore, RET was performed in the absence of NAD^+ and in the presence of DPI (typically ~14 μg ml^{-1} SMPs and 4 μM DPI, 32 °C, 2 min) to specifically modify any reduced flavin formed (27) and inactivate only those complexes I that are RET-competent; no NAD^+ reduction could be observed after DPI treatment, and increasing the DPI concentration or incubation time did not affect the results. Then, rotenone was added,

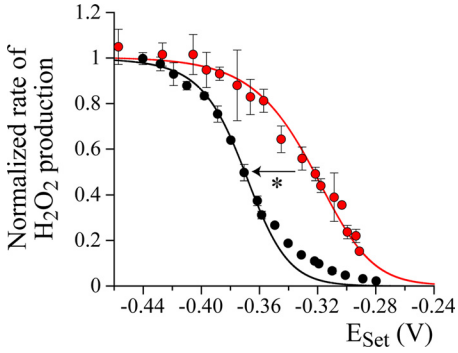

FIGURE 6. **Comparison of NADH- and RET-induced H_2O_2 production by complex I in SMPs.** The two curves have been normalized independently. *Black*, NADH-induced H_2O_2 production by complex I in SMPs inhibited by rotenone with $\Delta p \sim 0.16$ V (from Fig. 3). *Red*, RET induced H_2O_2 production by complex I in SMPs inhibited by KCN. The RET data are plotted using $E_{Set} = -0.020\ V - RT/2F \cdot \ln\{[succinate]/[fumarate]\} + 2.\Delta p$ (10 mM succinate, variable fumarate concentrations) and fit by the Nernst equation for a 2-electron cofactor with two distinct potentials described by their average value, $E_{av} = -0.305$ V, and their separation, $\Delta E = -0.020$ V. The rotenone independent rates (see Fig. 5) have been subtracted. The *asterisk* marks the 0.024 V increase in Δp (measured at $E_{1/2}$) that is required to overlay the RET-induced data on the NADH-induced data. See "Experimental Procedures" for conditions.

and the rate of NADH:$APAD^+$ oxidoreduction was compared with that from a control sample. In a typical preparation the rate decreased from 1.103 ± 0.007 to 0.975 ± 0.024 μmol min^{-1} mg of $protein^{-1}$, a decrease of 11.6%; only ~10% of the complex I present is RET-competent. Correcting the rate of RET-induced H_2O_2 production by complex I accordingly gives 1.51 ± 0.47 nmol min^{-1} mg of $protein^{-1}$, or ~20 min^{-1}. Thus, RET-induced H_2O_2 production is approximately three times slower than NADH-induced H_2O_2 production. Similarly, the corrected rate of RET-induced $APAD^+$ reduction is approximately three times slower than the rate of NADH-induced $APAD^+$ reduction. It is unlikely that the difference arises from kinetic limitations ($APAD^+$ reduction is significantly faster than O_2 reduction) but possible that the different mechanisms of flavin reduction (in forward and reverse) produce slightly different reduced states or that the positively charged DPI enhances the likelihood of flavin reduction. Changing the balance between $\Delta\psi$ and ΔpH (using 20 mM KCl with or without nigericin, see above) while maintaining the same Δp and external pH, does not affect RET-induced H_2O_2 production by complex I (see Fig. 5).

Finally, Fig. 6 compares the potential dependence of RET-induced H_2O_2 production by complex I in SMPs with that from NADH-induced H_2O_2 production in the presence of rotenone. The combination of Δp and the ubiquinone pool potential, imposed by succinate oxidation, provides a highly reducing potential, below −0.4 V. The RET- and NADH-induced data match well, except that the RET-induced dataset is shifted by 0.048 V relative to the NADH-induced dataset and broadened slightly. The data are shifted because the value of Δp used to calculate the set potentials during RET is an average over the whole population of SMPs, not just over those (with the highest Δp values) that are active in the RET assays. The two datasets can be overlaid by increasing the Δp value used to calculate the set potentials during RET by 0.048/2 V, indicating that the subpopulation of RET-competent SMPs exhibit an average Δp of 0.182 V. The broadening may reflect the absence of nucleotides in the RET experiment; as discussed previously (5), nucleotide binding affects the apparent titration curve of the flavin. Importantly, the RET-induced data vary over a region of potential that is consistent with the potential of the flavin in complex I (not with the potentials of any of the other cofactors (1) or with the potential dependence of a semiquinone). All these results are fully consistent with RET-induced H_2O_2 production being only from the reduced flavin in complex I.

DISCUSSION

A Unified Mechanism for Superoxide Production by Complex I under All Conditions during Both Forward and Reverse Electron Transfer—When ubiquinone reduction is prevented, and $\Delta p = 0$, complex I in SMPs behaves like isolated complex I (5); superoxide production is from the reduced flavin and determined by the NAD^+ and NADH concentrations (note that for simplicity we refer to superoxide production in our discussion, as it is the major species produced directly by complex I). When ubiquinone reduction is allowed, superoxide production slows in response to NADH oxidation; Q-site inhibitors do not stimulate it, but flavin-site inhibitors prevent it. No change in the behavior is observed when $\Delta p \sim 0.16$ V or when ΔpH is manipulated (at constant Δp and external pH). Therefore, there is no evidence for NADH-induced superoxide production from any site other than the reduced flavin. RET-induced superoxide production by complex I in SMPs is slower than NADH-induced superoxide production, although much of the difference can be attributed to heterogeneity in the SMPs, particularly to variation in Δp. The heterogeneity is a disadvantage of the SMP system; it can be described and taken into account but not fully characterized, and it offsets both the kinetics and thermodynamics of RET experiments. RET-induced superoxide production has a potential dependence consistent with the reduced flavin (not with a semiquinone); it is abolished by both Q-site and flavin-site inhibitors, and it is unaffected by manipulating ΔpH (at constant Δp and external pH). All the results are fully consistent with RET-induced superoxide production from the reduced flavin in complex I, and they provide no support for any additional site.

Comparison of Data from SMPs and Intact Mitochondria—The response of NADH-induced superoxide production to the NAD^+ potential in the matrix has been observed in intact mitochondria either by poising the NAD^+ potential (7) or by correlating the NAD(P)H fluorescence to superoxide production under a range of conditions (8, 13) (although fluorescence measurements evaluate the relative (NADH+NADPH) concentration, not the NAD^+ potential or absolute NADH concentration). The maximal rate of NADH-induced superoxide production by mitochondria (when complex I is inhibited and the NAD^+ pool is reduced) is typically equivalent to 0.4 nmol of H_2O_2 min^{-1} mg of $protein^{-1}$ (summarized in Ref. 41). Correcting for the mitochondrial antioxidant defenses (42) raises the value to ~1 nmol of H_2O_2 min^{-1} mg of $protein^{-1}$, and the fact that ~6% of the protein in *B. taurus* heart mitochondria is complex I (determined by comparison of the N2 EPR signal intensities in mitochondria (disrupted by either freezing or sonication and reduced by NADH) and an isolated complex I standard) gives a turnover number of ~17 min^{-1}. Finally, O_2 reduction by the reduced flavin is blocked by nucleotide binding, most strongly by NADH (6, 43) and, using the NADH-

concentration dependence from isolated complex I (6) with an estimated 1 mM NADH when the NAD^+ pool is reduced, gives ~11 min^{-1} for the SMPs. Given the estimations and approximations inherent to the comparison, the two values (SMPs 11 min^{-1}, 32 °C and mitochondria 17 min^{-1}, 37 °C) are fully consistent (although NADH-dependent contributions from matrix-localized dehydrogenases cannot be excluded (44, 45)). Conversely, during active RET (while NAD^+ is being reduced), the level to which the flavin is reduced is influenced by Δp and the ubiquinone potential as well as by the NAD^+ potential; the level of flavin reduction is not determined by the NAD^+ potential alone, so the NAD^+/NADH ratio and superoxide production need not correlate. Fluorescence measurements performed on mitochondria during RET have suggested that superoxide production is low as NAD(P)H accumulates, only becoming high once a constant level is established (13, 46). This observation is difficult to reconcile with superoxide production by a catalytic intermediate but consistent with RET-induced superoxide production being determined by the NAD^+ pool composition.

Brand and Lambert (10–12) proposed, from studies on intact mitochondria, that appropriate Q-site inhibitors "turn on" NADH-induced superoxide production by a semiquinone intermediate in complex I. Here, the effects of rotenone, piericidin A, and cyanide are all the same; they all simply inhibit NADH oxidation. In mitochondria, complex I Q-site inhibitors increase NADH-induced superoxide production (by preventing NADH oxidation and lowering the NAD^+ potential) but abolish RET-induced superoxide production (11, 12), consistent with superoxide production on the "NADH side" of the inhibitor binding site but not with an inhibitor-sensitive semiquinone. Furthermore, DPI, a characterized flavin site inhibitor (27), blocks RET-driven superoxide production in mitochondria (47, 48) as it does in SMPs.

It has been reported that ΔpH stimulates superoxide production by complex I in mitochondria, particularly during RET (10–12, 49). Notably, Lambert and Brand (11, 12) reported that ΔpH increases the apparent rate of RET-induced superoxide production (measured as H_2O_2) from ~0.4 nmol of H_2O_2 min^{-1} mg of $protein^{-1}$ (equal to the NADH-induced rate) to ~2.5 nmol of H_2O_2 min^{-1} mg of $protein^{-1}$, although the effect applies equally to NAD^+ reduction (at the flavin). Conversely, in SMPs, both NADH- and RET-induced superoxide production are independent of ΔpH, ruling out a direct effect of ΔpH on complex I itself. Importantly, SMPs allow the pH at the flavin site to be controlled precisely, independently of ΔpH, but in mitochondria the matrix pH can only be inferred from ΔpH, and abolishing ΔpH must decrease the matrix pH. Thus, we propose that the ΔpH effect is mediated by the matrix pH; it is known that NADH-induced superoxide production by isolated complex I increases significantly as the pH increases (5). pH-dependent kinetic and thermodynamic effects (particularly substrate and enzyme potentials) and other matrix dehydrogenases (44, 45) probably contribute also. Selivanov *et al.* (50) have suggested also that the apparent effects of ΔpH originate from increases in mitochondrial superoxide production as the matrix pH increases. Finally, reported rates of RET-induced superoxide production in mitochondria vary widely (summarized in Ref. 41), but they are generally considered to exceed rates of rotenone-inhibited NADH-induced superoxide production. The NAD^+ pool is highly reduced in both cases, but variations in the NAD^+ and NADH concentrations (7, 8) and especially differences in the redox status of the glutathione pool and the antioxidant capacity (42, 46) are further variables that determine the observed rates of superoxide production by both complex I and other enzymes (44, 45).

In summary, the flavin-site mechanism is sufficient to explain all extant data from studies of NADH- and RET-induced superoxide production by isolated complex I and complex I in SMPs, and these studies provide no support for any additional site. Interpreting the results of studies on isolated mitochondria is more challenging. First, although our mechanism should apply under all conditions, its direct application requires a more precise knowledge of the conditions (pH, nucleotide concentrations) that are relevant to each mitochondrial metabolic state than is currently available. Second, H_2O_2 detection in the mitochondrial systems depends on the balance between the intrinsic rate of superoxide production and the rates of detoxification (46). Finally, other matrix dehydrogenase enzymes may contribute to superoxide and H_2O_2 production by mitochondria, and the activity of complex I may be regulated or modified by additional effects such as protein modifications. Thus, the complex I flavin-site mechanism explains many of the characteristics of superoxide and H_2O_2 production by isolated mitochondria, and a more complete description will require a better understanding of both the conditions in the mitochondrion, and identification and characterization of additional effects and contributions that are present in mitochondria but absent from the experimental system used here.

Acknowledgments—We thank Alexander B. Kotlyar and Gary Cecchini for NADH-OH, Martin S. King for isolating complex I, Michael P. Murphy for helpful discussions, and Aleksandra Włodek for EPR spectroscopy.

REFERENCES

1. Hirst, J. (2010) *Biochem. J.* **425,** 327–339
2. Murphy, M. P. (2009) *Biochem. J.* **417,** 1–13
3. Raha, S., and Robinson, B. H. (2000) *Trends Biochem. Sci.* **25,** 502–508
4. Lin, M. T., and Beal, M. F. (2006) *Nature* **443,** 787–795
5. Kussmaul, L., and Hirst, J. (2006) *Proc. Natl. Acad. Sci. U.S.A.* **103,** 7607–7612
6. Birrell, J. A., Yakovlev, G., and Hirst, J. (2009) *Biochemistry* **48,** 12005–12013
7. Kushnareva, Y., Murphy, A. N., and Andreyev, A. (2002) *Biochem. J.* **368,** 545–553
8. Starkov, A. A., and Fiskum, G. (2003) *J. Neurochem.* **86,** 1101–1107
9. Sanz, A., Soikkeli, M., Portero-Otín, M., Wilson, A., Kemppainen, E., McIlroy, G., Ellilä, S., Kemppainen, K. K., Tuomela, T., Lakanmaa, M., Kiviranta, E., Stefanatos, R., Dufour, E., Hutz, B., Naudí, A., Jové, M., Zeb, A., Vartiainen, S., Matsuno-Yagi, A., Yagi, T., Rustin, P., Pamplona, R., and Jacobs, H. T. (2010) *Proc. Natl. Acad. Sci. U.S.A.* **107,** 9105–9110
10. Brand, M. D. (2010) *Exp. Gerontol.* **45,** 466–472
11. Lambert, A. J., and Brand, M. D. (2004) *J. Biol. Chem.* **279,** 39414–39420
12. Lambert, A. J., and Brand, M. D. (2004) *Biochem. J.* **382,** 511–517
13. Lambert, A. J., Buckingham, J. A., and Brand, M. D. (2008) *FEBS Lett.* **582,** 1711–1714
14. Smith, A. L. (1967) *Methods Enzymol.* **10,** 81–86
15. Kotlyar, A. B., and Vinogradov, A. D. (1990) *Biochim. Biophys. Acta* **1019,**

151–158
16. Beltrán, C., de Gómez-Puyou, M. T., Gómez-Puyou, A., and Darszon, A. (1984) *Eur. J. Biochem.* **144,** 151–157
17. Hansen, M., and Smith, A. L. (1964) *Biochim. Biophys. Acta* **81,** 214–222
18. Linnane, A. W., and Ziegler, D. M. (1958) *Biochim. Biophys. Acta* **29,** 630–638
19. Pullman, M. E., Penefsky, H. S., Datta, A., and Racker, E. (1960) *J. Biol. Chem.* **235,** 3322–3329
20. Jault, J. M., and Allison, W. S. (1993) *J. Biol. Chem.* **268,** 1558–1566
21. Votyakova, T. V., and Reynolds, I. J. (2004) *Arch. Biochem. Biophys.* **431,** 138–144
22. Orr, G. A., and Blanchard, J. S. (1984) *Anal. Biochem.* **142,** 232–234
23. Azzi, A., Montecucco, C., and Richter, C. (1975) *Biochem. Biophys. Res. Commun.* **65,** 597–603
24. Hille, R., and Massey, V. (1981) *J. Biol. Chem.* **256,** 9090–9095
25. Kotlyar, A. B., Karliner, J. S., and Cecchini, G. (2005) *FEBS Lett.* **579,** 4861–4866
26. Zharova, T. V., and Vinogradov, A. D. (1997) *Biochim. Biophys. Acta* **1320,** 256–264
27. Majander, A., Finel, M., and Wikström, M. (1994) *J. Biol. Chem.* **269,** 21037–21042
28. Kotlyar, A. B., and Vinogradov, A. D. (1984) *Biochim. Biophys. Acta* **784,** 24–34
29. Huang, L. S., Sun, G., Cobessi, D., Wang, A. C., Shen, J. T., Tung, E. Y., Anderson, V. E., and Berry, E. A. (2006) *J. Biol. Chem.* **281,** 5965–5972
30. Vinogradov, A. D., and Grivennikova, V. G. (2005) *Biochemistry* **70,** 120–127
31. Bason, J. V., Runswick, M. J., Fearnley, I. M., and Walker, J. E. (2011) *J. Mol. Biol.* **406,** 443–453
32. Chance, B., and Hollunger, G. (1960) *Nature* **185,** 666–672
33. Ksenzenko, M., Konstantinov, A. A., Khomutov, G. B., Tikhonov, A. N., and Ruuge, E. K. (1983) *FEBS Lett.* **155,** 19–24
34. Sled, V. D., Rudnitzky, N. I., Hatefi, Y., and Ohnishi, T. (1994) *Biochemistry* **33,** 10069–10075
35. Yakovlev, G., and Hirst, J. (2007) *Biochemistry* **46,** 14250–14258
36. Reda, T., Barker, C. D., and Hirst, J. (2008) *Biochemistry* **47,** 8885–8893
37. Rottenberg, H., and Lee, C. P. (1975) *Biochemistry* **14,** 2675–2680
38. Bashford, C. L., and Thayer, W. S. (1977) *J. Biol. Chem.* **252,** 8459–8463
39. O'Rourke, B. (2007) *Annu. Rev. Physiol.* **69,** 19–49
40. Sorgato, M. C., Ferguson, S. J., Kell, D. B., and John, P. (1978) *Biochem. J.* **174,** 237–256
41. Hirst, J., King, M. S., and Pryde, K. R. (2008) *Biochem. Soc. Trans.* **36,** 976–980
42. Treberg, J. R., Quinlan, C. L., and Brand, M. D. (2010) *FEBS J.* **277,** 2766–2778
43. Grivennikova, V. G., and Vinogradov, A. D. (2006) *Biochim. Biophys. Acta* **1757,** 553–561
44. Starkov, A. A., Fiskum, G., Chinopoulos, C., Lorenzo, B. J., Browne, S. E., Patel, M. S., and Beal, M. F. (2004) *J. Neurosci.* **24,** 7779–7788
45. Grivennikova, V. G., Kareyeva, A. V., and Vinogradov, A. D. (2010) *Biochim. Biophys. Acta* **1797,** 939–944
46. Aon, M. A., Cortassa, S., and O'Rourke, B. (2010) *Biochim. Biophys. Acta* **1797,** 865–877
47. Liu, Y., Fiskum, G., and Schubert, D. (2002) *J. Neurochem.* **80,** 780–787
48. Lambert, A. J., Buckingham, J. A., Boysen, H. M., and Brand, M. D. (2008) *Biochim. Biophys. Acta* **1777,** 397–403
49. Zoccarato, F., Cavallini, L., Bortolami, S., and Alexandre, A. (2007) *Biochem. J.* **406,** 125–129
50. Selivanov, V. A., Zeak, J. A., Roca, J., Cascante, M., Trucco, M., and Votyakova, T. V. (2008) *J. Biol. Chem.* **283,** 29292–29300